TABLE 1 Gain, Beamwidth, and Beam Direction at Different Frequencies

Frequency (GHz)	Gain (dBi)	E-Plane Beam-Peak Angle	E-Plane Half-Power Beamwidth	H-Plane Beam-Peak Angle	H-Plane Half-Power Beamwidth
11.7	22.6	14.5°	15.4°	−0.5°	5.15°
12	22.9	15°	15.7°	−0.5°	5.11°
12.2	23.5	15°	15.3°	0°	5.5°
12.5	23.8	15°	15°	0°	5.1°
12.7	23.1	15.5°	14.3°	0°	4.5°

used are air ($\varepsilon_r = 1$, height = 1 mm) and Rogers Corporation RO4003 ($\varepsilon_r = 3.38$, height = 0.2 mm). The element spacing of the cavity-backed microstrip patch is $0.8\lambda_0$. To obtain the required bandwidth of the element, the total height of the cavity-backed microstrip patch element is 3 mm. The height of the microstrip line is 1 mm in order to reduce the radiation leakage from the microstrip line. The subarray, as shown in Figure 1, is interconnected 12 elements by three series-feeds and two parallel-feeds. The series-feed is designed as short as possible to reduce the disadvantage and preserve the advantage of the series-feed. All elements are designed to have uniform power distribution for high gain. To achieve such a power division, the impedance of the line is controlled, as shown in Figure 5. The impedance matching is considered at every junction on the transmission lines. To fix the main beam 15° away from the broadside direction, the feed phase of each patch layer from bottom to top direction in Figure 1 is 0°, 77.4°, 154.8°, and 232.2° as shown in Figure 6. The performance of the proposed array is fairly agrees with that of calculated.

3. ARRAY PERFORMANCE

The measured two principal-plane patterns are presented in Figure 7. The half-power beamwidth in E-plane [Fig. 7(a)] and H-plane [Fig. 7(b)] is about 15° and 5°, respectively. The main beam is directed 15° away from the broadside direction, as shown in Figure 7(a). In general, the reflected wave is added at junctions in the parallel feed. However, the input phase differences for 15° beam tilting result in a decrease of the reflected wave at some of junctions [4]. Figure 8 shows the measured return loss measured at the input port. The loss due to the tilted beam is small (cos15° = 0.9659). Table 1 shows the gain, beamwidth, and direction of main beam at different frequencies. At the center frequency (12.5 GHz), the measured gain is 23.8 dBi, while the calculated directivity is 24.44 dBi. The return loss of the input port is 20 dB. The loss due to the microstrip transmission feed in the array is only 0.59 dB (87.4% efficiency). Total efficiency is 83.3%. The good antenna efficiency is mainly due to the adequate combination of corporate and series feeds. Figure 9 shows the proposed antenna array mounted on the rooftop of the vehicle.

Figure 9 Photograph of the proposed array antenna mounted on the rooftop of the vehicle. [Color figure can be viewed in the online issue, which is available at www.interscience.wiley.com.]

4. CONCLUSION

By adopting the combined corporate and series feeds, a high-efficiency and relatively wide bandwidth microstrip array in the Ku-band has been developed and manufactured for mounting in a vehicle. Low profile and manufacturing cost are also achieved. The elevation angle of the beam is controlled electrically rather than mechanically to achieve a low profile of the antenna array. The beam is scanned in the azimuth plane by the mechanical tracking system rather than the phased array system with phasor shifters in order to minimize the antenna's manufacturing cost.

ACKNOWLEDGMENT

This work is supported by the Ministry of Information & Communication of Korea ("Support Project of University Information Technology Research Center" supervised by IITA).

REFERENCES

1. L. Ely and M. Gabi, A study of microstrip array antennas with the feed network, IEEE Trans Antennas Propagat 37 (1989), 426–434.
2. G. Kang, H. Lee, J. Kim, N. Kim, B. Lee, and J. Lee, Wideband dual linearly polarized patch array antenna, Proc ISAP Yokusuka, Japan (2002), 225–228.
3. J. Huang, A Parallel-series-fed microstrip array with high efficiency and low cross-polarization, Microwave Opt Technol Lett 5 (1992), 230–233.
4. T. Tasuku, M. Tanaka, and W. Chujo, Wideband circularly polarized array antenna with sequential rotations and phase shift of elements, Proc ISAP Kyoto, Japan (1985), 117–120.

BROADBAND RECTANGULAR-TO-RIDGE-TO-T-SEPTUM WAVEGUIDE TRANSFORMERS

Vladimir A. Labay[1] and Jens Bornemann[2]
[1] Department of Electrical and Computer Engineering
Gonzaga University
Spokane, WA 99258
[2] Department of Electrical and Computer Engineering
University of Victoria
Victoria, BC, Canada V8W 3P6

Received 15 April 2004

ABSTRACT: *Broadband transformers from rectangular to T-septum waveguides are presented. By utilizing both ridge and T-septum waveguide sections in the transformer design, the thicknesses of the ridge and the T-septa can be kept constant, which simplifies fabrication. The three- and four-section designs achieve relative bandwidths of 57% and 72%, respectively. Both designs are verified through computations with commercially available field solver software.* © 2004 Wiley Periodicals, Inc. Microwave Opt Technol Lett 43: 183–185, 2004; Published online in Wiley InterScience (www.interscience.wiley.com). DOI 10.1002/mop.20414

Key words: *T-septum waveguide; ridge waveguide; waveguide transformers*

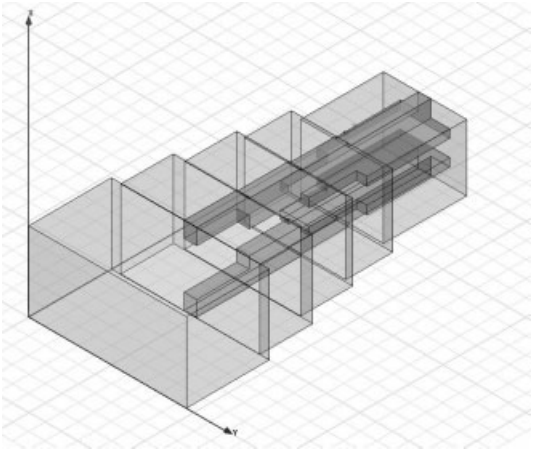

Figure 1 Broadband rectangular-to-ridge-to-T-septum waveguide transformer

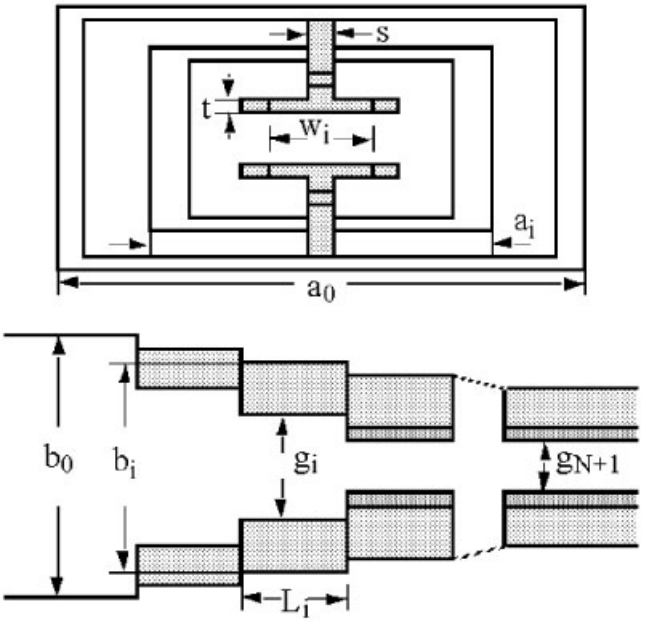

Figure 2 Front view (top) and side view (bottom) of the rectangular-to-ridge-to-T-septum waveguide transformer

1. INTRODUCTION

The limited monomode bandwidth of rectangular waveguides is commonly increased by inserting longitudinal metal-ridge [1–3], T-shaped [4, 5], or L-shaped [6, 7] septa. In order to connect such waveguides to standard measurement equipment, waveguide transformers are required to facilitate increased bandwidth due to a cross-sectional single- or double-plane field symmetry known from waveguide feed systems (see, for example, [8]). For ridge waveguides, broadband transformers have been designed using transmission-line theory [9] and full-wave approaches [10]. They are realized by sandwiching a stepped ridge between the two halves of a stepped waveguide housing. Whereas high-power transformers require the ridge thickness to be different in every transformer section [9], regular applications can be designed with a constant ridge thickness [10], which allows for a simpler fabrication process.

With the demonstrated capability of T-septum waveguide technology towards smaller components and broadband performance, for example, in [11–14], a certain demand for rectangular-to-T-septum waveguide transformers exists. The only transformer designed thus far [14] exclusively uses T-septum transformer sections, which complicates the fabrication process due to varying septa dimensions between the individual transformer stages.

Therefore, this paper focuses on the design of novel broadband rectangular-to-T-septum waveguide transformers (Fig. 1), which also uses ridged sections to maintain constant ridge and T-septum thickness, thus easing the manufacturing process of the entire septa.

2. DESIGN PROCESS

The cross-section and side views of the input/output and transformer sections are depicted in Figure 2. For given cross-section dimensions of the input/output ports and related performance specifications in terms of midband frequency, bandwidth, and return loss, the impedance profile of the transformer is obtained according to standard practices (see, for example, [8]). In the next step, a stepped profile of the housing ($a_i \times b_i$ in Fig. 2) is selected; it can be linear or exponential, or follow a similar function. For given constant ridge s and T-septum thickness t, the gap width g (for a ridged section) and the width w (for a T-septum waveguide section) are designed to match the individual section's impedances. This is performed with a 2D routine based on the mode-matching technique (MMT) and subdomain basis functions [13]. As long as the impedance can be achieved with $g_i \geq g_{N+1}$, the respective section will be a ridge waveguide. Otherwise, the section will be a T-septum waveguide with $g_i = g_{N+1}$, and the width w_i will be increased to meet the impedance. All individual sections should have a cutoff frequency close to that of the feeding waveguide. In the case where this condition collides with the impedance requirement, the housing dimensions in this section can be modified. The section lengths L_i are initially selected to be one-quarter of the guided wavelength.

The final design step consists of two stages in which an MMT routine similar to that of [13] and an optimization strategy [15] are used. In the first optimization run, only the section lengths are optimized. This works towards adjusting the initial quarter-wave section lengths in order to account for the fringing fields. The second optimization includes parameters a_i, b_i, g_i, w_i, and L_i ($0 < i < N + 1$) and respects the above constraints that a ridge guide needs to be used whenever $g_i \geq g_{N+1}$ and that s and t remain constant.

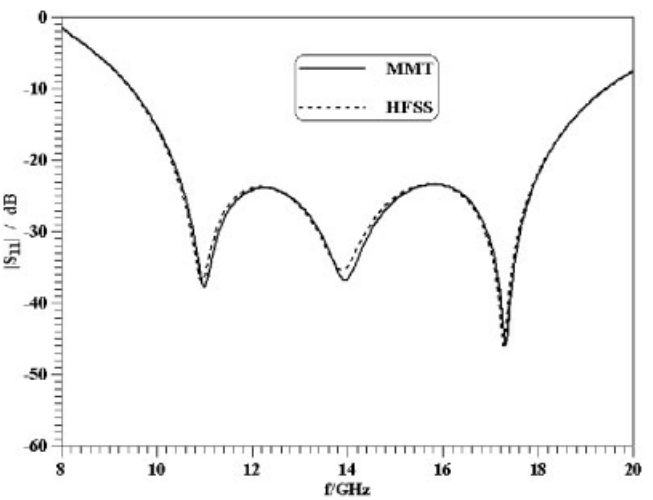

Figure 3 Performance of three-section broadband rectangular-to-ridge-to-T-septum waveguide transformer (for dimensions, see Table 1)

3. RESULTS

The design examples presented here involve a T-septum waveguide of cross-sectional dimensions $a_{N+1} = 10$ mm, $b_{N+1} = 8$ mm, $w_{N+1} = 6$ mm, $g_{N+1} = 2$ mm, $s = 1.5$ mm, and $t = 1$ mm (see Fig. 2). Comparing the cutoff frequency of this cross section with those of standard guides, a WR 75 waveguide (19.05×9.525 mm) was selected as the feed.

Figure 3 shows the performance of a three-section transformer involving two ridge waveguide sections and one T-septum section. The dimensions are listed in Table 1. This design achieves a 20-dB return-loss bandwidth of 57%. The return loss is better than 23 dB over a 54% bandwidth. As shown in Figure 3, excellent agreement with the calculations of the commercial software package HFSS is obtained, thus verifying the design procedure.

In order to further improve the bandwidth, a four-section transformer was designed for the same input and output dimensions (see Table 1). Figure 4 shows the computed performance featuring bandwidths of 72% and 70% for 20-dB and 23-dB return loss, respectively. Although the return-loss evaluation with HFSS reveals some discrepancy with our MMT design, especially above 15 GHz, the broadband behavior of this transformer is confirmed. The difference in return-loss ripple is 23 dB with the MMT, as compared to 18.7 dB with HFSS, which is still sufficient for a wide range of broadband-transformer applications.

4. CONCLUSION

Broadband transitions from rectangular to T-septum waveguides can be designed by using both ridge and T-septum sections as transformers. Compared to a previous design, this procedure simplifies the fabrication of the septa, which in turn makes it less sensitive to manufacturing tolerances. Basic design guidelines have been presented, and two broadband-transformer examples have achieved bandwidths of 57% and 72%. These designs, which are based on MMT routines, have been verified by the commercial software package HFSS.

TABLE 1 Dimensions in mm of Three- and Four-Section Transformers Presented in Figs. 3 and 4 ($s = 1.5$ mm, $t = 1.0$ mm)

Dimensions	Three-Section Design	Four-Section Design
a_0	19.0500	19.0500
b_0	9.5250	9.5250
a_1	16.7472	17.7429
b_1	9.3928	9.2874
g_1	5.6394	6.0552
L_1	6.3444	6.0745
a_2	13.9765	14.1164
b_2	9.1498	9.2436
g_2	2.8278	3.6558
L_2	6.2840	6.8446
a_3	12.1995	12.0830
b_3	8.7248	9.0414
g_3	2.0000	2.0218
w_3	3.5207	—
L_3	5.6866	5.8837
a_4	10.0000	10.3428
b_4	8.0000	8.5620
g_4	2.0000	2.0000
w_4	6.0000	4.0923
L_4	output	5.9999
a_5	—	10.0000
b_5	—	8.0000
g_5	—	2.0000
w_5	—	6.0000
L_5	—	output

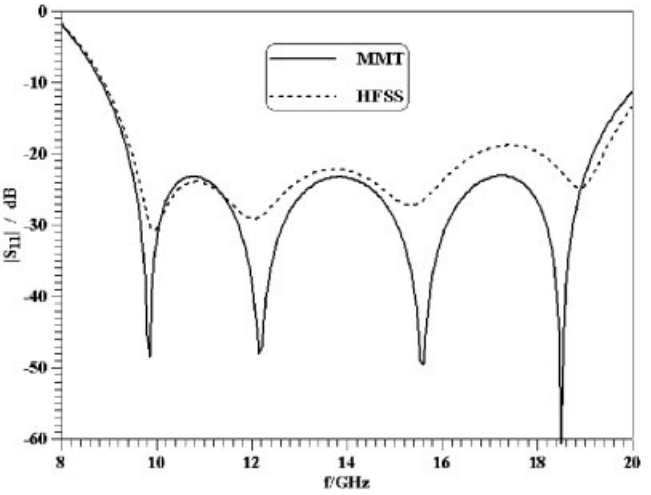

Figure 4 Performance of four-section broadband rectangular-to-ridge-to-T-septum waveguide transformer (for dimensions, see Table 1)

REFERENCES

1. S. Hopfer, The design of ridged waveguides, IRE Trans Microwave Theory Tech 3 (1955), 20–29.
2. J.P. Montgomery, On the complete eigenvalue solution of ridged waveguide, IEEE Trans Microwave Theory Tech 19 (1971), 547–555.
3. W. Sun and C.A. Balanis, Analysis and design of quadruple-ridged waveguides, IEEE Trans Microwave Theory Tech 42 (1994), 2201–2207.
4. Y. Zhang and W.T. Jones, Some properties of T-septum waveguides, IEEE Trans Microwave Theory Tech 35 (1987), 769–775.
5. P.K. Saha and G.G. Mazumder, Bandwidth characteristics of inhomogeneous T-septum waveguides, IEEE Trans Microwave Theory Tech 37 (1989), 1021–1026.
6. P.K. Saha and D. Guha, New broadband rectangular waveguide with L-shaped septa, IEEE Trans Microwave Theory Tech 40 (1992), 777–781.
7. P.K. Saha and D. Guha, Bandwidth and dispersion characteristics of a new rectangular waveguide with two L-shaped septa, IEEE Trans Microwave Theory Tech 47 (1999), 87–92.
8. J. Uher, J. Bornemann, and U. Rosenberg, Waveguide components for antenna feed systems: Theory and CAD, Artech House, Norwood, MA, 1993.
9. E.S. Hensperger, Broadband stepped transformers from rectangular to double-ridged waveguide, IRE Trans Microwave Theory Tech 6 (1958), 311–314.
10. J. Bornemann and F. Arndt, Modal *S*-matrix design of metal finned waveguide components and its application to transformers and filters, IEEE Trans Microwave Theory Tech 40 (1992), 1528–1537.
11. V.A. Labay and J. Bornemann, CAD of T-septum waveguide evanescent-mode filters, IEEE Trans Microwave Theory Tech 41 (1993), 731–733.
12. V.A. Labay and J. Bornemann, An integrated T-septum waveguide diplexer for compact front-end applications, 1993 IEEE MTT-S Int Symp Atlanta, GA, 1993, pp. 463–466.
13. V.A. Labay, J. Bornemann, S. Amari, and J.M. Damaschke, Direct-coupled waveguide filters for the lower gigahertz frequency range, Int J RF Microwave CAE 12 (2002), 217–225.
14. V.A. Labay, Computer-aided design of passive microwave components in nonstandard rectangular waveguide technology, Ph.D. Thesis, University of Victoria, Victoria, BC, Canada, 1995.
15. K. Madsen, H. Schaer-Jacobsen, and J. Voldby, Automated minimax design of networks, IEEE Trans Circ Syst 22 (1975), 791–796.